

Electronic and Optical Properties of GaAs Armchair Nanoribbons: DFT Approach

Bramha P. Pandey

Department of Electronics & Communication Engineering, MMMUT, Gorakhpur(U.P)-273010.

Received 23 August 2017; Revised 1 November 2017; Accepted 20 December 2017

ABSTRACT

The electronic and optical properties of N atom-width ($N: 4, 8, 12, 16$) armchair GaAs nanoribbons (NA GaAs NRs) have been studied with hydrogen (H) passivated nanoribbons using the DFT approach. The H passivated edge of NA GaAs NRs with different widths of nanoribbons provide great flexibility to modulate the fundamental band gap. All investigated width of 4, 8, 12, and 16 atom GaAs NRs are found to be semiconducting with direct band gaps of 3.071, 2.275, 2.155, and 2.02 eV respectively at k -point Z (0, 0, 0.5), which exhibit interesting width dependent ($N: 4\sim 12$) behaviour of the band gap. The complex dielectric constant was calculated using the Kubo-Greenwood formula, from which the refractive index($n(\omega)$) and absorption coefficient ($\alpha(\omega)$) were also calculated for the bulk as well as for all width of GaAs armchair nanoribbons. The n_{zz} and α_{zz} components significantly play a major role in tuning the refractive index and optical absorption coefficient of the GaAs nanoribbons.

Keywords Nanoribbon(NR), Armchair, DFT, MGGA, Absorption Coefficient, Refractive Index, Bandgap.

1. INTRODUCTION

Two-dimensional (2D) materials such as graphene and other variants of graphene are playing a vital and exciting role in the field of high-speed nano devices since the last decade [1]–[3]. In particular, graphene has attracted great interest because of its unique properties; pristine graphene exhibits metallic behaviour with no band gap, whereas modified graphene can have a finite band gap. The band gap is critical to devices such as switching diodes, light emitting diodes, photodetectors, and solar cells. Different approaches have been adopted on graphene to modulate the band gap, such as graphene nanoribbon synthesis [4], bilayer control [5], [6] and chemically modified graphene[7]–[9]. However, most of these efforts have failed to achieve a significant variation in the band gap of graphene[10]. The 2D non-graphene materials including layered, non-layered, and the heterostructures are presently appealing and are having increased attention due to their favorable applications in electronics, optoelectronics and clean energy, and nanodevices [11], [12]. 2D non-graphene materials are fabricated with the same efficiency and performance as graphene, which opens a new dimension for research such as the monolayer transition metal disulfide (TMD), which are likely complementary materials of graphene[13]–[17].

Recently, wavy GaAs nanoribbons were fabricated onto a strained soft substrate to investigate the strain–photonic coupling effect [18], [19]. The electronic and transmission properties of a low buckled GaAs nanoribbon have been investigated [20]. In the present work, we report the

first-principle calculations of band gap modulation and optical properties such as the refractive index and the absorption coefficient in NA GaAs NRs by passivating the nanoribbon edges with a hydrogen atom using the density functional theory (DFT). In engineering, band structure, optical properties, and boundary modification of the nanoribbons are a promising and vital option. The most commonly used edge passivation is hydrogenation. The As edge of NA GaAs NRs is passivated with a hydrogen atom, which leads to the bonding of As atoms at the edges, different than the other As atoms that are bonded to Ga. Consequently, the bond length of As-H at the edges are shorter than that in the middle of the GaAs ribbons, thus opening the energy gaps of the armchair NA GaAs NRs. The dangling bonds at the armchair edges play a vital role in governing the electronic and optical properties. The rate of the side of nanoribbon hydrogenation is determined by the temperature, pressure, and concentration of H₂ in the passivation process[21]. The most favourable condition (i.e., As edges are terminated with H) has been considered for the hydrogenation of the NA GaAs NRs. When the nanoribbon is passivated with a hydrogen atom, excess As that can be present either in elemental form or as an oxide As₂O₃, can be removed by the reaction mechanism[22]. The objective of this study is to design hydrogen (H) passivated armchair GaAs nanoribbons to analyse the electronic (band gap, band structure), and optical (Refractive index, Absorption coefficient) properties of armchair GaAs nanoribbons, taking into consideration four different widths (N: 4, 8, 12, and 16) of nanoribbons.

2. COMPUTATIONAL DETAILS

The armchair GaAs nanoribbon structures can be viewed as tailoring a GaAs crystal in the (100) Miller direction with a padding of 10 Å vacuum in the x and y-direction while z is periodic and perpendicular to the armchair direction. Accordingly, the so-called armchair GaAs nanoribbons (NA GaAs NRs) can be identified by the number of layers of atoms across the ribbon width and are labelled as NA GaAs NRs. In this work, we focus on the armchair type and shown in Figure 1, is the ball-and-stick model of NA GaAs NRs. We consider four different NA GaAs NRs with N = 4, 8, 12, and 16, which correspond to a width of 5.65 Å, 11.31 Å, 16.96 Å, and 22.61 Å respectively. Upon structural relaxations, the lattice constants along the periodic direction were calculated to be 4.05 Å, 3.99 Å, 3.98 Å, and 3.96 Å respectively. The atomic structure of NA GaAs NRs shows the low-buckled honeycomb lattice structure after the relaxation of the unit cell [23].

The relaxation calculations were carried out using the first principles density functional theory (DFT) implemented in the quantum espresso source code [24]. The interaction between electrons and ions is defined by the Perdew-Burke-Ernzerhof (PBE) exchange-correlation functional [25] and the ultra soft pseudopotential (USPP) [26]. The kinetic energy and charge density cut offs for the plane wave basis set were chosen at 50 Ry and 650 Ry respectively.

The energy convergence criterion for electronic and ionic iterations were set at 10⁻⁶ eV and 10⁻⁴ eV, respectively. The force convergence threshold was selected at 10⁻³ eV/Å in the ionic relaxation of the atoms for NA GaAs NRs. The reciprocal space was meshed at 1 × 1 × 16 for the NA GaAs NRs using Monkhorst Pack meshes centred at Γ point[27]. A vacuum space of at least 10 Å was included in the unit cell to minimize the interaction between the system and its periodic replicas that resulted from the periodic boundary condition. The electronic and optical properties of the relaxed structure of NA GaAs NRs were calculated using the meta GGA(MGGA) method implemented in the quantum-wise simulation tool[28]. The MGGA functional combined with the Tran and Blaha (TB09) method is a semi-empirical approach to accurately predict the electronic band structure and the optical spectrum of the materials[29]. The calculation of the electronic and optical properties requires a good description of virtual states far above the Fermi level.

Therefore, we used the Hartwigsen, Goedecker, Hutter (HGH) pseudopotentials[30] with 4 Tier basis function for all atoms present in the unit cell. The K-points sampling and density mesh cut off for basic functions were selected as 1x1x64 Monkhorst Pack mesh grid and 100 Ha respectively. The 1x1x128 K-points mesh was included in the band structure and the optical spectrum calculations.

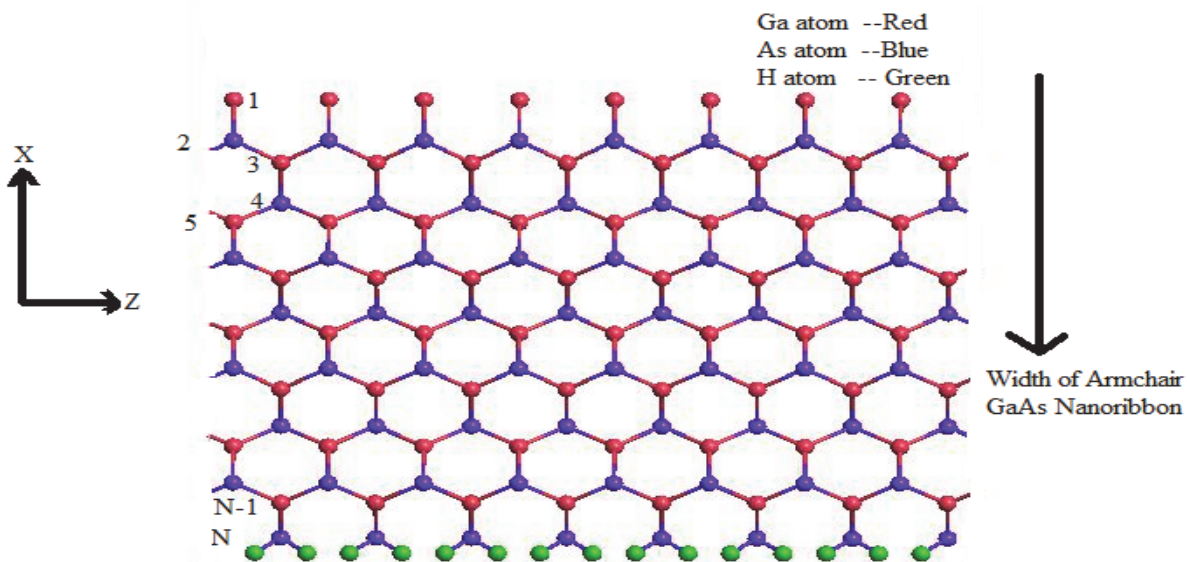


Figure 1. Basic structure of a buckled armchair GaAs nanoribbon.

3. RESULTS AND DISCUSSION

3.1 Electronic Properties Calculation

All calculations were performed after the optimization of the unit cell of different widths of hydrogen atom passivated NA GaAs NRs. The calculated band gap of bulk zincblende GaAs was found to be 1.41 (1.42) eV by using the MGGA functional and setting the empirical parameter $c=1.162$. The value of the empirical parameter c was calculated using self-consistent DFT calculations employed in the ATK-DFT code. A GaAs NRs was confined in two dimensions and periodic in the z-direction. Therefore the unit cell became anisotropic structure. Due to the change in structure from isotropic (bulk GaAs) to anisotropic (NA GaAs NRs), the valence band maximum and the conduction band minimum k-point were shifted to Z from Γ . It is interesting to note that at Z, there is a valence band maximum and a conduction band minimum, termed as the direct band gap and is shown in Figure 2 (a, b). The direct band gap of all studied NA GaAs NRs was calculated and tabulated in Table 1. There is a plausible flexibility to tune the NA GaAs NRs band gap by changing the width of the GaAs nanoribbons.

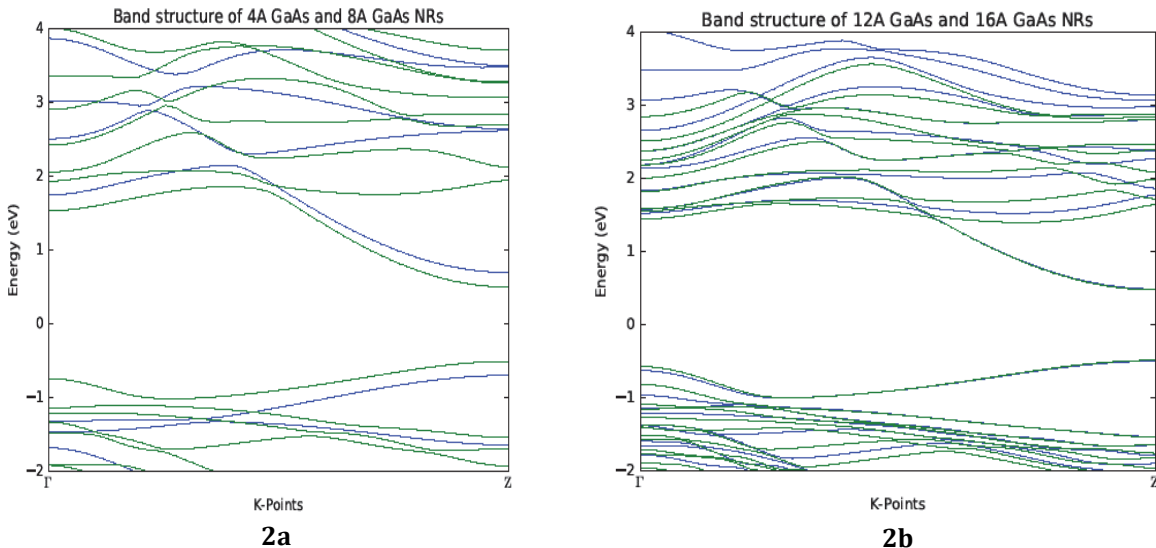


Figure 2a and 2b. Show the band structure of N (4, 8), and N (12, 16) armchair GaAs nanoribbons respectively. The band structure of 4A GaAs and 8A GaAs NRs were plotted in Figure 2a with blue and green colour respectively. Figure 2b shows the band structure of 12A GaAs and 16A GaAs NRs with blue and green colour respectively. The calculated band structures of NA GaAs NRs predict the direct band gap nature of NA GaAs NRs at Γ (gamma) and decrease as the width of GaAs nanoribbons increases.

3.2 Optical Properties Calculation

The optical properties were calculated with the calculation susceptibility tensor, $\chi(\omega)$ by using the Kubo-Greenwood formula[31]. The relative dielectric constant $\epsilon_r(\omega)$, polarizability $p(\omega)$, and optical conductivity, $\sigma(\omega)$, are related to the susceptibility $\chi(\omega)$ as:

$$\epsilon_r(\omega) = (1 + \chi(\omega)), \quad p(\omega) = V\epsilon_0\chi(\omega), \quad \text{and} \quad \sigma(\omega) = -i\omega\epsilon_0\chi(\omega), \text{ respectively [32].}$$

The refractive index, n , is related to the complex dielectric constant through

$$n + ik = \sqrt{\epsilon_r}$$

where the refractive index and extinction coefficients are n and k , respectively. The n and k are represented in the form of real (ϵ_1) and imaginary (ϵ_2) components of the complex dielectric constant as

$$n(\omega) = \sqrt{\frac{\epsilon_1^2 + \epsilon_2^2 + \epsilon_1}{2}} \quad \text{and} \quad k(\omega) = \sqrt{\frac{\sqrt{\epsilon_1^2 + \epsilon_2^2} - \epsilon_1}{2}}$$

The optical absorption coefficient is represented in the form of the extinction coefficient (k),

$$\alpha(\omega) = 2 \left(\frac{\omega}{c} \right) k$$

where the speed of light, angular frequency, and extinction coefficient are c , ω , and k , respectively[33].

From the optimized structure of bulk zincblede GaAs, we calculated the refractive index, $n(\omega)$ and optical absorption coefficient, $\alpha(\omega)$ as a function of the incident photon wavelength(λ) shown in Figure 3. The calculated average values of the refractive index, $n(\omega)$ over the whole

range of wavelength is ~ 3.1 (experimental 3.2 [34]) of bulk zincblende GaAs. It is noticeable that $n(\omega)$ and $\alpha(\omega)$ are equal in all directions because the bulk GaAs is an isotropic and periodic crystal. The NR GaAs NRs were optimized and the $n(\omega)$ and $\alpha(\omega)$ were calculated as a function of the incident photon λ shown in Figure 4, 5, 6 and 7 respectively for all N widths (4, 8, 12, and 16). For all widths of GaAs NRs, the average refractive index is ~ 1.5 . The $n(\omega)$ and $\alpha(\omega)$ became an anisotropic crystal due to the confinement in the x and y -direction and periodic in the z -direction. We found different values of $n(\omega)$ in the n_{xx} , n_{yy} , and n_{zz} direction for all four nanoribbon widths. Similarly, $\alpha(\omega)$ is the combination of all three different direction components α_{xx} , α_{yy} and α_{zz} for all four nanoribbon widths. It was also observed that as the nanoribbon's width increases from 4 to 16, the z - direction components become more dominating compared with the other two components of $n(\omega)$ and $\alpha(\omega)$. It happened because all NA GaAs NRs are periodic in the z -direction and had sufficient vacuum padded in the x and y -direction so that the periodic replicas of the structure cannot interact with each other. The modulation of $n(\omega)$ and $\alpha(\omega)$ is possible by changing the width of NA GaAs NRs. The n_{zz} and α_{zz} components significantly play the major role in tuning the refractive index and optical absorption coefficient of the GaAs nanoribbons.

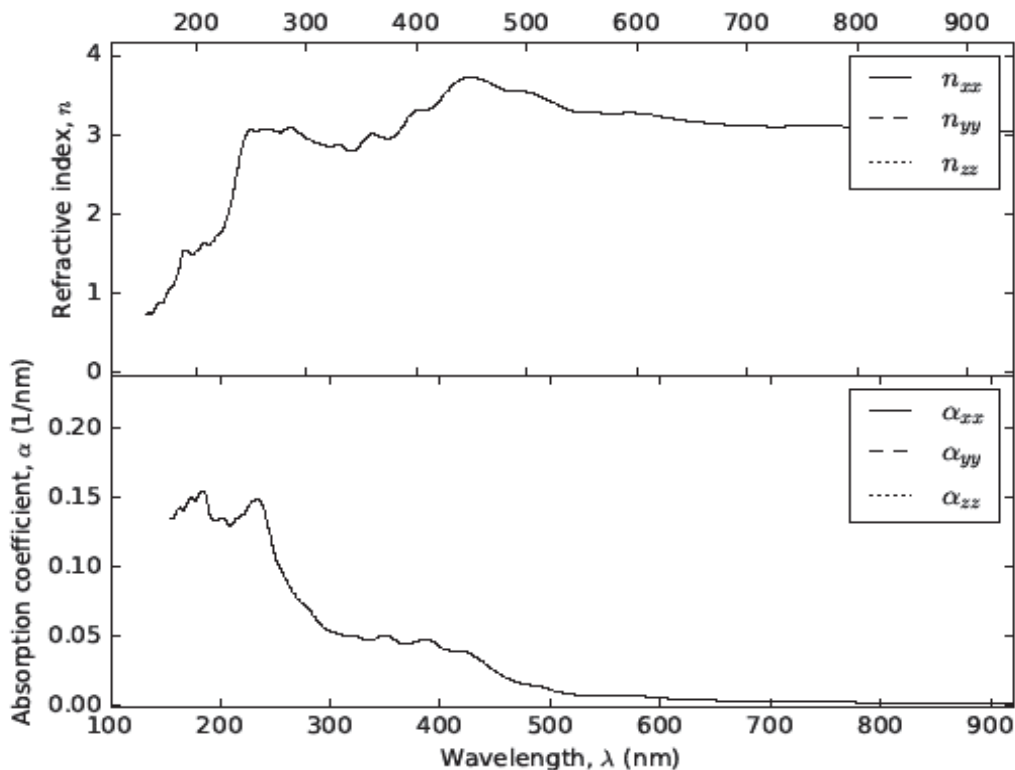


Figure 3. Refractive index $n(\omega)$ and absorption coefficient $\alpha(\omega)$, calculated with complex dielectric constant for bulk zinc-blende GaAs.

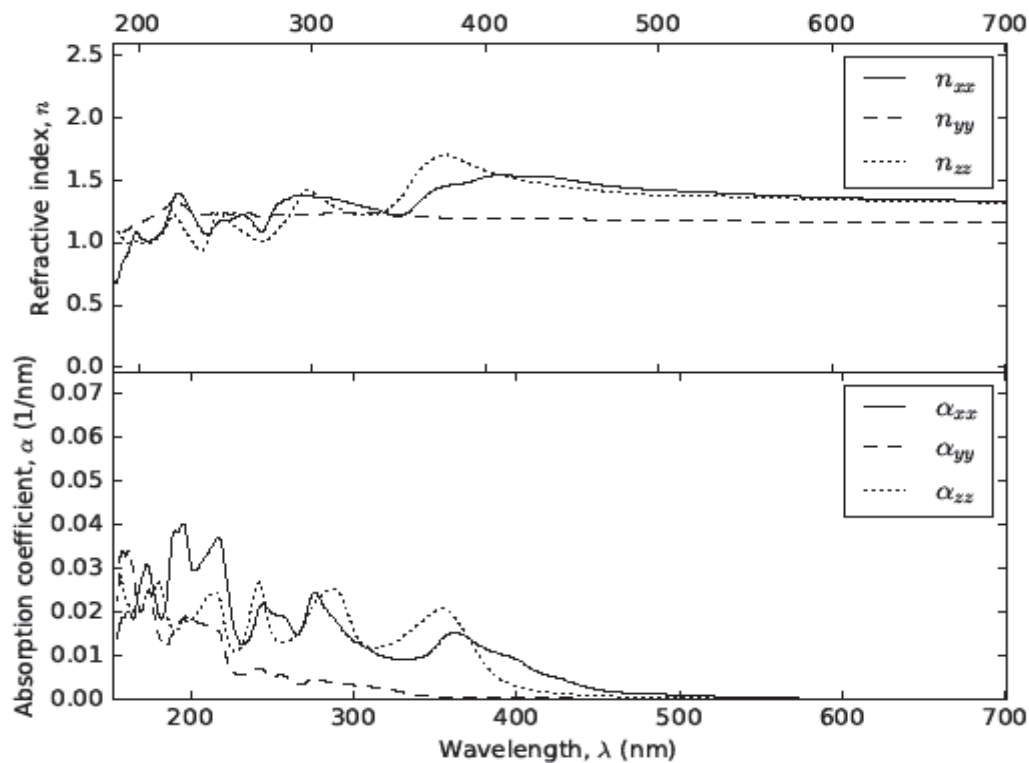


Figure 4. Refractive index $n(\omega)$ and absorption coefficient $\alpha(\omega)$, calculated with complex dielectric constant for 4A GaAs NR.

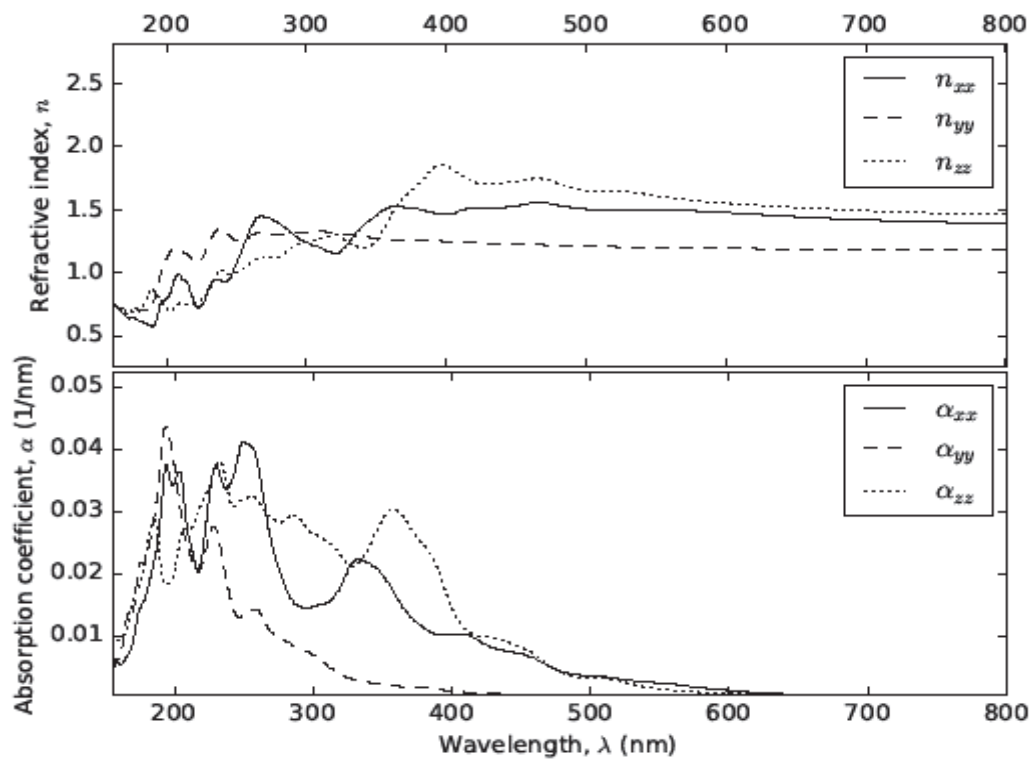


Figure 5. Refractive index $n(\omega)$ and absorption coefficient $\alpha(\omega)$, calculated with complex dielectric constant for 8A GaAs NR.

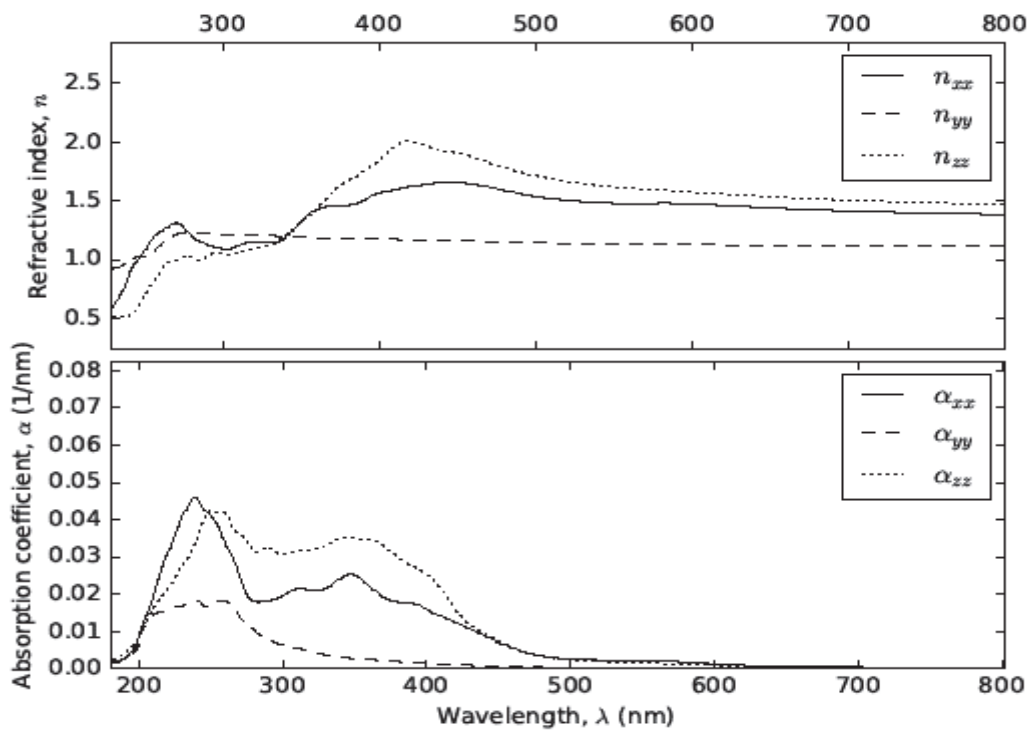


Figure 6. Refractive index $n(\omega)$ and absorption coefficient $\alpha(\omega)$, calculated with complex dielectric constant for 12A GaAs NR.

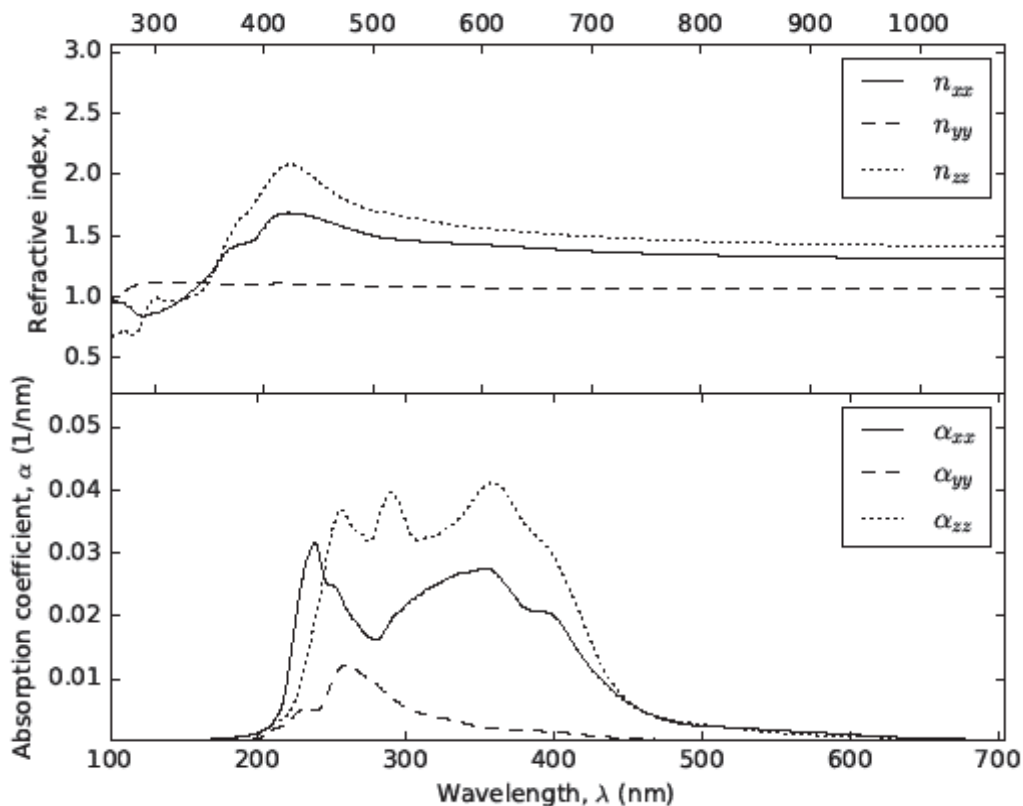


Figure 7. Refractive index $n(\omega)$ and absorption coefficient $\alpha(\omega)$, calculated with complex dielectric constant for 16A GaAs NR.

4. CONCLUSION

In the present work, hydrogen (H) passivated armchair GaAs nanoribbons were designed and the electronic and optical properties of NA GaAs NRs were calculated with the help of the DFT theory. The modulation of the bandgap is possible by varying the width of the NA GaAs NRs as shown in Table 1. The optical properties were calculated using the Kubo-Greenwood formula, from which the refractive index and absorption coefficient were calculated for the bulk as well as for all widths of GaAs armchair nanoribbons. The refractive index $n(\omega)$ and the optical absorption coefficient $\alpha(\omega)$ of the GaAs nanoribbons can be significantly modulated by varying the widths of the GaAs nanoribbons. The most governing component of the refractive index and optical absorption coefficient are n_{zz} and α_{zz} respectively.

Table 1 Bandgap (in eV) of NA GaAs NRs with different widths ($N = 4, 8, 12, 16$). The band gap of bulk GaAs has been calculated and compared with the experimental results

Structure NA GaAs NRs	Fundamental direct bandgap (Z- Z)	Experimental Bandgap
Bulk GaAs	1.41	1.42[35]
4A GaAs NR	3.071	
8A GaAs NR	2.275	
12A GaAs NR	2.155	
16A GaAs NR	2.02	

ACKNOWLEDGEMENT

The author would like to thank IUAC, Delhi and C-DAC, Pune for providing the high-performance computing facility available at IUAC and C-DAC center for this research article.

REFERENCES

- [1] Y. Zhu, *et al.*, "Graphene and graphene oxide: Synthesis, properties, and applications," *Adv. Mater.* **22**, 35 (2010) 3906.
- [2] A. Splendiani, *et al.*, "Emerging photoluminescence in monolayer MoS₂," *Nano Lett.* **10**, 4, (2010) 1271.
- [3] F. Bonaccorso, Z. Sun, T. Hasan, A. C. Ferrari, "Graphene Photonics and Optoelectronics," *Nat. Photonics* **4**, 9 (2010) 611.
- [4] J. Cai, *et al.*, "Atomically precise bottom-up fabrication of graphene nanoribbons," *Nature*, 466, 7305 (2010) 470.
- [5] T. Ohta, "Controlling the Electronic Structure of Bilayer Graphene," *Science (80)* **313**, 5789 (2006) 951.
- [6] J. B. Oostinga, H. B. Heersche, X. Liu, A. F. Morpurgo, L. M. K. Vandersypen, "Gate-induced insulating state in bilayer graphene devices," *Nat. Mater.* **7**, 2 (2008) 151.
- [7] X. Dong, *et al.*, "Symmetry breaking of graphene monolayers by molecular decoration," *Phys. Rev. Lett.* **102**, 13 (2009).
- [8] K. Novoselov, V. Fal, L. Colombo, "A roadmap for graphene," *Nature*, **490**, 7419 (2012) 192.
- [9] D. C. Elias, *et al.*, "Control of graphene's properties by reversible hydrogenation: evidence for graphane," *Science (80-.)* **323**, 5914, (2009) 610.

- [10] K. Kim, J.-Y. Choi, T. Kim, S.-H. Cho, H.-J. Chung, "A role for graphene in silicon-based semiconductor devices," *Nature*, **479**, 7373 (2011) 338.
- [11] F. Wang, *et al.*, "Synthesis, properties and applications of 2D non-graphene materials," *Nanotechnology*, **26**, 29 (2015) 292001.
- [12] B. Santhibhushan, M. Soni, A. Srivastava, "Optical properties of boron-group (V) hexagonal nanowires: DFT investigation," *Pramana - J. Phys.* **89** (2017) 14.
- [13] S. Das, H. Y. Chen, A. V. Penumatcha, J. Appenzeller, "High performance multilayer MoS₂ transistors with scandium contacts," *Nano Lett.* **13**, 1, 92013(100).
- [14] W. Zhang, *et al.*, "Ultrahigh-gain photodetectors based on atomically thin graphene-MoS₂ heterostructures," *Sci. Rep.* **4** (2014) 3826.
- [15] M. Bernardi, M. Palummo, J. C. Grossman, "Extraordinary sunlight absorption and one nanometer thick photovoltaics using two-dimensional monolayer materials," *Nano Lett.* **13**, 8 (2013) 3664.
- [16] T. Roy, *et al.*, "Field-effect transistors built from all two-dimensional material components," *ACS Nano* **8**, 6 (2014) 6259.
- [17] B. Radisavljevic, A. Kis, "Mobility engineering and a metal-insulator transition in monolayer MoS₂," *Nat. Mater.* **12**, 9, (2013) 815.
- [18] Y. Wang, *et al.*, "Buckling-Based Method for Measuring the Strain-Photonic Coupling Effect of GaAs Nanoribbons," *ACS Nano* **10**, 9 (2016) 8199.
- [19] C. Sealy, "GaAs nanoribbons take the strain," *Nano Today* **11**, 5 (2016) 539.
- [20] B. P. Pandey, "Electronic and Transmission Properties of Low Buckled GaAs Armchair Nanoribbons," *J. Surf. Sci. Technol.* **33**, 3 (2017) 91.
- [21] B. Mahler, V. Hoepfner, K. Liao, G. A. Ozin, "Colloidal synthesis of 1T-WS₂ and 2H-WS₂ nanosheets: Applications for photocatalytic hydrogen evolution," *J. Am. Chem. Soc.* **136**, 40 (2014) 14121.
- [22] A. A. Balmashnov, K. S. Golovanivsky, E. M. Omeljanovsky, A. V Pakhomov, A. Y. Polyakov, "Passivation of GaAs by atomic hydrogen flow produced by the crossed beams method," *Semicond. Sci. Technol.* **5** (1990) 242.
- [23] H. Şahin *et al.*, "Monolayer honeycomb structures of group-IV elements and III-V binary compounds: First-principles calculations," *Phys. Rev. B - Condens. Matter Mater. Phys.* **80**, 15 (2009).
- [24] P. Giannozzi *et al.*, "QUANTUM ESPRESSO: a modular and open-source software project for quantum simulations of materials," *J. Phys. Condens. Matter* **21**, 39 (2009) 395502.
- [25] J. Perdew, K. Burke, Y. Wang, "Generalized gradient approximation for the exchange-correlation hole of a many-electron system," *Phys. Rev. B* **54**, 23 (1996) 16533.
- [26] K. Laasonen, R. Car, C. Lee, and D. Vanderbilt, "Implementation of ultrasoft pseudopotentials in ab initio molecular dynamics," *Phys. Rev. B* **43**, 8 (1991) 6796.
- [27] H. J. Monkhorst, J. D. Pack, "Special points for Brillouin-zone integrations," *Phys. Rev. B* **13**, 12 (1976) 5188.
- [28] "Atomistix ToolKit version 2016, 2, QuantumWise A/S (www.quantumwise.com).
- [29] F. Tran, P. Blaha, "Accurate Band Gaps of Semiconductors and Insulators with a Semilocal Exchange-Correlation Potential," *Phys. Rev. Lett.* **102** (2009) 226401.
- [30] C. Hartwigsen, S. Goedecker, J. Hutter, "Relativistic separable dual-space Gaussian pseudopotentials from H to Rn," *Phys. Rev. B* **58** (1998) 3641.
- [31] W. A. Harrison, *Solid state theory*. New York: McGraw-Hill, 1970.
- [32] R. M. Martin, "Electronic Structure: Basic Theory and Practical Methods," *Book.* (2004) 624.
- [33] D. J. Griffiths, *Introduction to Electrodynamics*, 3rd ed. New Jersey: Prentice Hall, 1999.
- [34] B. Herrmann, *Synthetic Methods of Organometallic and Inorganic Chemistry*, 2nd ed. New York: Georg Thieme Verlag Stuttgart, 1996.
- [35] S. Adachi, *Handbook on Physical Properties of Semiconductors*. chichester: John Wiley & Sons, 2005.

